# Occlusion-robust Detector Trained with Occluded Pedestrians

Zhixin Guo, Wenzhi Liao, Peter Veelaert and Wilfried Philips

*Ghent University-IMEC, Sint-Pietersnieuwstraat 41, Gent 9000, Belgium*

Keywords: Pedestrian Detection, Occlusion Handling, Adaboost, Integral Channel Features.

Abstract: Pedestrian detection has achieved a remarkable progress in recent years, but challenges remain especially when occlusion happens. Intuitively, occluded pedestrian samples contain some characteristic occlusion appearance features that can help to improve detection. However, we have observed that most existing approaches intentionally avoid using samples of occluded pedestrians during the training stage. This is because such samples will introduce unreliable information, which affects the learning of model parameters and thus results in dramatic performance decline. In this paper, we propose a new framework for pedestrian detection. The proposed method exploits the use of occluded pedestrian samples to learn more robust features for discriminating pedestrians, and enables better performances on pedestrian detection, especially for the occluded pedestrians (which always happens in many real applications). Compared to some recent detectors on Caltech Pedestrian dataset, with our proposed method, detection miss rate for occluded pedestrians are significantly reduced.

## 1 INTRODUCTION

Pedestrian detection is a key problem in computer vision and has numerous applications including video surveillance, self-driving vehicles and robotics. Many tasks such as pedestrian tracking and semantic understanding rely heavily on the performance of pedestrian detectors. Although it has been intensively studied during the past several decades, occlusion remains challenging.

Because of the significant success of the deformable part-based models (DPM) approach (Felzenszwalb et al., 2010), many researchers work on this model to overcome the occlusion issues. Instead of conventionally treating pedestrians as a whole object (Dalal and Triggs, 2005), DPM models separate a pedestrian into different body parts. The occluded parts can then be handled properly and the influence of changed appearance caused by occlusion is eliminated. But this requires an accurate estimation of the visibility of different body parts (Wang et al., 2009; Ouyang et al., 2016), which makes the training of DPM models delicate and complex. Besides, the high computation cost of training a set of detectors from different body parts and fusion of their detection scores further increase the difficulties of this kind of methods.

Through observation of the Caltech Pedestrian dataset (Dollar et al., 2012), Dollar et al. indicate that most occluded pedestrians have a limited number of occlusion types (7 types account for 97% of all occlusions in the dataset). Inspired by this discovery, some researchers train a set of occlusion-specific models to improve the detection of occluded pedestrians (Mathias et al., 2013). However, this method suffers from similar problems as the DPM based methods. Training distinct detectors for different occlusion patterns is not only costly, but also difficult because of the need for a sufficient number of specific occluded pedestrian samples. In addition, a proper method to merge the results of distinct detectors is also needed, because the occlusion pattern is unknown during detection.

In summary, most current approaches do not use occluded pedestrians during the training stage, because detectors cannot distinguish a real pedestrian from the occluding object, which results in learning wrong parameters and causes a significant performance drop. Some methods (Wojek et al., 2011; Mathias et al., 2013) introduce occluded pedestrians into the training procedure, but these samples are classified into different occlusion patterns and only the visible regions are actually used when training the occlusion-specific detectors.

Inspired by the idea that some valuable appearance characteristics in occluded pedestrian samples could be used to enhance the detector's occlusion-handling performance, we propose a new framework that makes full advantage of the occlusion information for training. The main contributions of this paper are as follows. 1) We exploit occluded pedestrian

Guo, Z., Liao, W., Veelaert, P. and Philips, W.
Occlusion-robust Detector Trained with Occluded Pedestrians.
DOI: 10.5220/0006569200860094
In *Proceedings of the 7th International Conference on Pattern Recognition Applications and Methods (ICPRAM 2018)*, pages 86-94
ISBN: 978-989-758-276-9

samples into the training stage to further improve the detection performances. 2) We propose a new feature selection strategy based on the occlusion distribution of the training samples. Experimental results on the Caltech Pedestrian dataset demonstrate that the detection performance of our approach significantly exceeds the performance of some existing methods.

The rest of the paper is organized as follows. After reviewing the related work in Section 2, we introduce the baseline ACF detector and our proposed method in Section 3 and Section 4 respectively. Section 5 shows the experimental results. The conclusion is drawn in Section 6.

## 2 RELATED WORK

Over the past decades a great effort has been made to improve the pedestrian detection performance. In this section, we first discuss the development of the boosted detection framework on which we base our work, and then review the state-of-the-art occlusion-handling methods.

In 2004, Viola and Jones (Viola and Jones, 2004) pioneered a detection architecture that computed features very efficiently with integral images. Adaboost (Friedman et al., 2000) was used to train a cascade of decision trees, and a sliding window strategy was employed to search each potential region of the image. This successful structure was then combined with some more powerful features. Dalal and Triggs (Dalal and Triggs, 2005) proposed the histogram of oriented gradient (HOG) feature which since then has been widely used. Some researchers combined HOG with additional features (Walk et al., 2010; Wang et al., 2009), while the integral channel features (ICF) proposed by Dollar et al. (Dollár et al., 2009) showed excellent discriminative power. In the ICF detector, the VJ boosted structure (Viola and Jones, 2004) is used to select appropriate ICF features and train powerful classifiers. Inspired by the ICF architecture, a variety of improvements have been made to achieve better performance as well as efficiency. FPDW (Dollár et al., 2010) detector is proposed to accelerate the detection by estimating some features across different image scales, instead of computing them explicitly. Benenson et al. (Benenson et al., 2012) move this estimation from the detection to the training stage and further improve efficiency. To strengthen the representation ability of features, SquaresChnFtrs (Benenson et al., 2013) uses all sizes of square feature pools instead of random rectangular pools and get better performance. More recently, Dollar et al. (Dollár et al., 2014) proposes the ACF detector, which far outperforms contemporary detectors. Based on ACF, LDCF (Nam et al., 2014) demonstrates that decorrelation of local feature information is helpful. Some recent work continues to improve the detection performance by generalizing more powerful features (Zhang et al., 2015), exploring the model capacity (Ohn-Bar and Trivedi, 2016) or combining detectors with deep Convolutional Neural Network (CNN) models (Angelova et al., 2015).

For occlusion-handling, it is natural to first estimate the visibility of pedestrian body parts, and then handle the visible and occluded parts separately. Wang et al. (Wang et al., 2009) propose to use the response of HOG features of the global detector to estimate the occlusion likelihood map. The final decision is made by applying the pre-trained part detectors on the fully visible regions. To further explore the visibility correlations of body parts, Ouyang et al. (Ouyang et al., 2016) employ a deep network, which supplements the DPM detection results. In (Enzweiler et al., 2010), Enzweiler et al. obtain the degree of visibility by examining occlusion discontinuities extracted from additional depth and motion information.

Since it is rather hard to ensure the accuracy of visibility estimation, some researchers turn to the training of a set of distinct detectors for different occlusion patterns. In (Wojek et al., 2011), a full-body DPM detector and six part-based detectors, at low and high resolution, are trained and combined to make the final decision. While in (Mathias et al., 2013), Mathias et al. train a more exhaustive set of ICF detectors (16 different occlusion patterns). By biased feature selection and reusing trained detectors, the training cost can be 10 times lower compared to conventional brute-force training. Besides single-person models, some multi-person occlusion patterns are investigated to handle occlusion in crowded street scenes. Tang et al. (Tang et al., 2014) make use of the characteristic appearance pattern of person-person occlusion, and train a double-person detector for occluded pedestrian pairs in the crowd. A similar model is proposed in (Ouyang and Wang, 2013b) where the authors use a probabilistic framework instead of Non-maximum Suppression (NMS) to deal with strong overlaps.

Enlightened by the ideas in (Tang et al., 2014) and (Ouyang and Wang, 2013b) that occlusion can be used as valuable information rather than as a distraction, we propose a new framework for pedestrian detection. This method explicitly makes use of the occluded pedestrian samples, which may contain useful occlusion appearance information, but are mostly discarded by existing methods.

# 3 BASELINE DETECTOR AND DATASET

## 3.1 Aggregate Channel Feature (ACF) Detector

ACF (Dollár et al., 2014) employs a boosting structure that greedily minimizes a loss function for the final decision rule

$$F(\mathbf{x}) = \sum_t \alpha_t f_t(\mathbf{x}), \tag{1}$$

where the strong classifier $F(\mathbf{x})$ is a weighted sum of $t$ weak classifiers $f_t(\mathbf{x})$. $\alpha_t$ denotes the weight of each weak classifier, and $\mathbf{x} \in R^K$ is the feature vector. In ACF, the channel features (Dollár et al., 2009) are used, including 6 histogram of oriented gradient channels, 1 gradient magnitude channel and 3 LUV colour channels. A given image is transformed into 10 channels of per-pixel feature maps. Given an input feature $\mathbf{x} \in R^K$, a decision tree acts as a weak classifier and outputs the confidence score $f_t(\mathbf{x})$.

A weak decision tree is built during each iteration of the training procedure. At each non-leaf node of the tree, a binary decision stump will be learned. The main task of training a decision stump is selecting one feature from a set of candidate features (pixels) and exhaustively searching its optimal threshold values. The feature (with its corresponding threshold) which leads to the smallest classification error will be selected. The classification error at one stump is a weighted summation of the misclassified samples:

$$\varepsilon = \sum \omega_i \mathbf{1}_{\{f(\mathbf{x}_i) \neq y_i\}}, \tag{2}$$

where $\mathbf{1}_{\{...\}}$ is the indicator operator. $f(\mathbf{x}_i)$ and $y_i$ indicate the classification result and true class of the input feature $\mathbf{x}_i$ respectively. $\omega_i$ is the weight of each training sample. Given a feature index $k \in \{1, 2, ..., K\}$, the classification error of a given feature is:

$$\varepsilon_{(k)} = \sum_{\mathbf{x}_i[k] \leq \tau} \omega_i \mathbf{1}_{\{y_i = +p\}} + \sum_{\mathbf{x}_i[k] > \tau} \omega_i \mathbf{1}_{\{y_i = -p\}}, \tag{3}$$

where $\mathbf{x}_i[k]$ indicates the $kth$ feature of the sample $\mathbf{x}_i$. $\varepsilon_{(k)}$ indicates the classification error when selecting the $kth$ feature and threshold $\tau$. $p$ is a polarity element $\{\pm 1\}$. By greedily learning all the stumps, a decision tree is built. The default ACF detector is composed of 4096 such trees with a maximum depth of 5.

The above training structure has been proved to be very effective for non-occluded pedestrians. However, during the selection of optimal features, only the classification error is taken into consideration. This sole judgement standard makes the selection susceptible to noisy image patches, and in particular, to the occlusion of pedestrian samples. In the following section we will propose a more robust feature selection strategy that better exploits the occluded pedestrian samples.

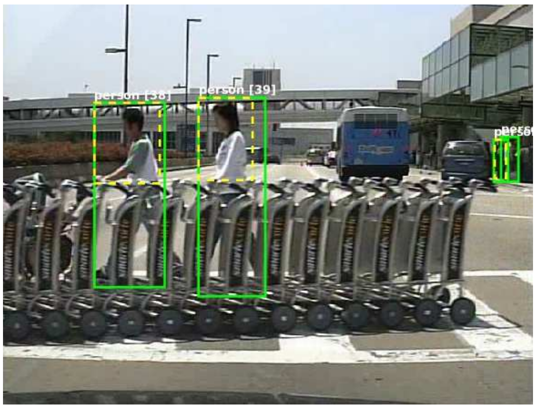

Figure 1: Caltech Pedestrian Dataset.

## 3.2 Caltech Pedestrian Dataset

In our experiments, we use the Caltech Pedestrian dataset (Dollar et al., 2012), which is currently one of the most popular pedestrian detection benchmarks. It consists of 250k labeled frames with 350k annotated bounding boxes. In particular, each partially occluded pedestrian is annotated with two bounding boxes (see Fig. 1), which indicate the full body (in green) and the visible part (in yellow) respectively. This visible region information will be used for the training with occluded pedestrians in Section 4.3.

# 4 PROPOSED METHOD

This section details our proposed method on how to introduce the occluded pedestrian samples into the training stage and improve the detection performances of the occluded pedestrians. Specifically, we first assume that all the training samples have the same known occlusion region (Fig. 2(a)) in Section 4.1, then we extend this assumption to a more realistic situation and propose a biased feature selection strategy in Section 4.2. Last but not least, we apply the proposed feature selection strategy to the real situation and propose a new training structure for the occluded pedestrians in Section 4.3.

In ACF detector, the final decision is made by a combination of weak classifier results. Each weak classifier will read several pixels from the feature map (Fig. 2(b)). The key insight of this paper is that we can improve the detection by controlling the feature selection procedure during the training of decision trees.

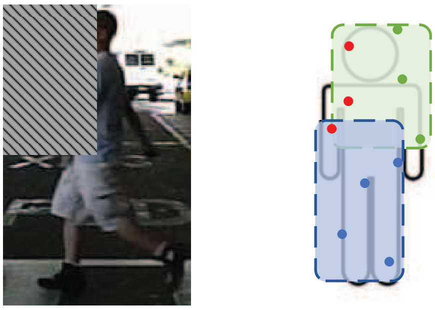

(a) (b)

Figure 2: Pedestrian samples are manually occluded in the top-left corner with non-person image patches randomly cut from negative samples. Some features in the occlusion region (marked as red) are selected by weak classifiers but they are not reliable.

To simplify this problem, a default setting of the ACF detector is applied to demonstrate the validity of our proposed method, while a more exhaustive exploration of the detector and the best performance can be found in Section 5.

## 4.1 Simple Situation: Known Occlusions

We start with the very simple case, where we assume that all samples have the same occlusion region in the top-left corner (the occlusion region occupies 1/4 of the image area, see Fig. 2(a)). This is the easiest case to handle because we are certain that features that are located in the occluded region do not represent characteristics of pedestrians. Thus if the features selected by weak classifiers are in the top-left corner of the feature map (red pixels in Fig. 2(b)), they must be unreliable. What we need to do is to just restrict the locations of features, forbidding the selection of features in the occlusion region.

We simulate this simple case by covering all the training samples (including positive and negative samples) with non-pedestrian image patches in the top-left corner. These image patches are randomly cut from the negative samples. In Fig. 3(a) we can see the feature distribution of the model trained by our manually occluded samples. As expected, although the detector selects most of the features from the non-occluded region, a few features from the top-left corner are also used. Therefore, we also train a new model in which we forbid the selection of features in the top-left corner. In Fig. 4, *simple* and **simple* indicate the performance of the original ACF model and the new ACF model without using the features of occluded regions, while **simple* outperforms *simple* both in the reasonable and the partial occlusion cases.

Therefore, we can improve the detection by avoiding the selection of unreliable features during the training stage. We may presume the features in the top-left corner to be unreliable because all samples have the same occlusion in that area. However, for more complex situations, it will be more difficult to judge the reliability of a feature.

## 4.2 Complex Situation: Training with Sample Mixtures

Now we assume a more complex and realistic situation that only 20% of the samples are occluded in the top-left corner. The features in the occluded region can no longer be discarded directly because they undergo a little influence from the occlusion but still represent some pedestrian characteristics. Therefore, instead of judging a feature only by the classification error (as explained in Section 3.1), we need an additional selection criterion that takes into account the occlusion probability of a feature during the training stage. In short, if two features from the input feature map have very similar classification errors, we prefer the one that has lower occlusion probability. Therefore, we propose a new method to select features, of which a new cost function $\varepsilon'_{(k)}$ (feature $k$ is selected) can be defined:

$$\varepsilon'_{(k)} = \varepsilon_{(k)}(1+\gamma_{(k)}) \tag{4}$$

$$\gamma_{(k)} = \theta * (N^{occ}_{(k)}/N^{pos}_{(k)}) \tag{5}$$

where $\varepsilon_{(k)}$ indicates the classification error defined in Eq. (3), $\gamma_{(k)}$ represents the occlusion cost coefficient of feature $k$, which increases its classification error according to its occlusion probability $N^{occ}_{(k)}/N^{pos}_{(k)}$. $N^{pos}_{(k)}$ indicates the number of positive samples in the current node, while $N^{occ}_{(k)}$ indicates the number of samples that have an occlusion in the location of feature $k$. $\theta$ acts as a constant weight to control the impact of the occlusion cost. To ensure that the classification error is always the prior consideration, we set the $\theta$ value much smaller than 1 (In this paper we have made multiple experiments and finally set 1/25 as the $\theta$ value. A bigger $\theta$ will overweight the occlusion probability and sacrifice some very discriminative features) so that a feature with low occlusion probability will be preferred to a feature that is barely better but has much higher occlusion probability. Hence a feature is selected according to the new classification cost:

$$k = argmin\ \varepsilon'_{(k)} \tag{6}$$

In this part $N^{occ}_{(k)}/N^{pos}_{(k)}$ equals 0.2 and 0 for features in the occlusion and non-occlusion regions, respectively. Fig. 3(b) shows a biased feature selection

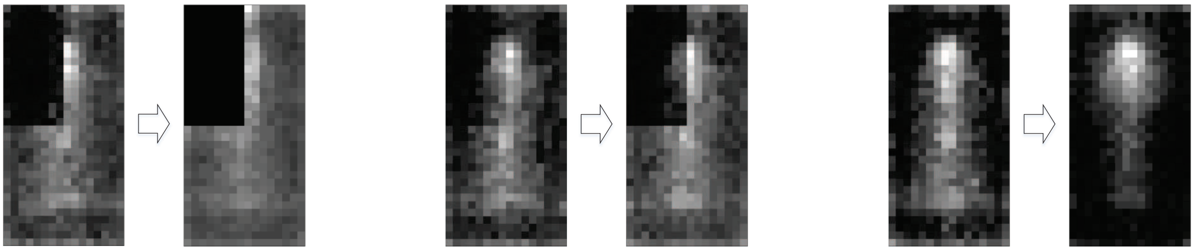

(a) Simple situation: avoid selecting features in the occlusion region

(b) Complex situation: features in the occlusion region are assigned bigger classification cost which lower the probability of being selected

(c) Real situation: the combination of the new classification cost with occlusion distribution map makes the feature selection more biased on low probability occlusion regions

Figure 3: Distribution of the feature selection rate in trained models. Features in the brighter area are more likely to be selected.

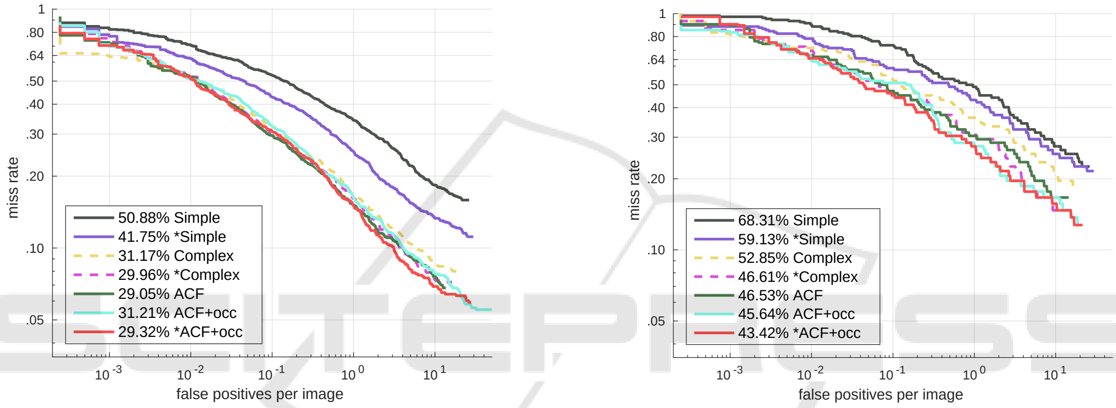

(a) Reasonable

(b) Partial occlusion

Figure 4: Performance of models trained in different situations. (a) Reasonable: less than 35% occluded pedestrians (including full-visible ones) (b) Partial occlusion: less than 35% occluded pedestrians (excluding full-visible ones).

of the modified model that fewer features in the top-left corner are selected. In Fig. 4, we use *complex* and **complex* to indicate the performances of the original model (trained with original feature selection strategy of Eq. (3)) and the modified model (trained with the proposed feature selection strategy of Eq. (4) and (5)), respectively. The modified model **complex* shows an improvement from 31.17% to 29.96% (lower log-average miss rate indicates better performance) in the reasonable case (Fig. 4(a)) and an improvement from 52.85% to 46.61% in the partial occlusion case (Fig. 4(b)). In addition, we can find that the modified model **complex* has achieved comparable performance to that of the default ACF model trained with non-occlusion pedestrian samples (29.05% and 46.53%).

So far we have only focused on the manually specified occluded samples whose occlusion regions are fixed. For real pedestrian samples, we need to handle the occlusion which may occur in any part of a person.

### 4.3 Real Situation

Now we propose a new method to take advantage of the real occluded pedestrian samples during the training stage. This method is based on the new feature selection strategy proposed in Section 4.2, where the occlusion probability of a feature is taken into account by introducing a modified cost function (Eq. (4) and (5)). Unlike the manually occluded samples used in Section 4.1 and 4.2, the occlusion regions of real samples are unfixed. Therefore, the occlusion probability of feature $k$ $N^{occ}_{(k)}/N^{pos}_{(k)}$ in Eq. (5) is no longer a constant. We will estimate it by calculating the occlusion distribution map of the training samples.

We create a binary 16×32 pixel occlusion mask map for each occluded pedestrian sample marked with visible bounding boxes. By averaging all the marked samples, we obtain an occlusion distribution map in Fig. 5(a). From the map we notice that the occlusion distribution is not uniform. The lower part of a pedestrian is more likely to be occluded while the

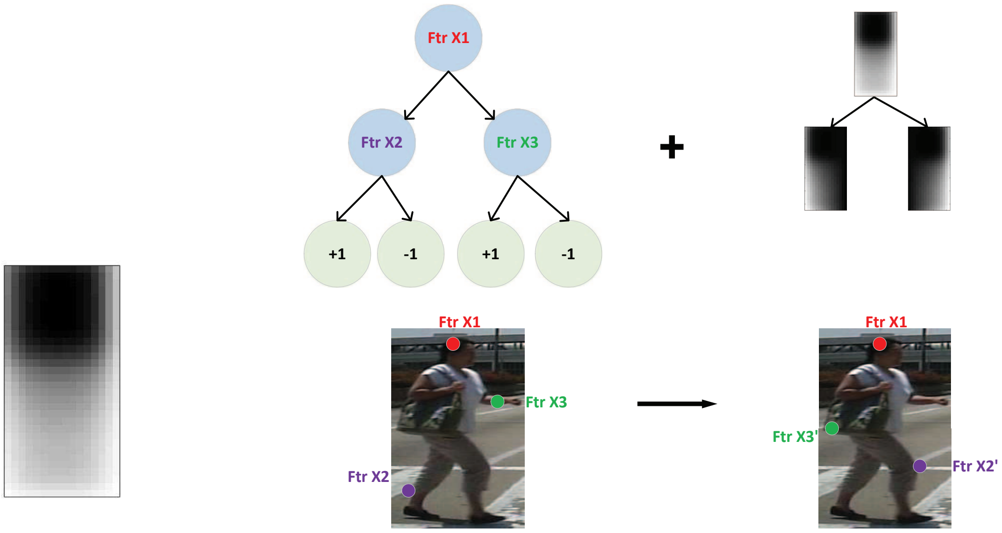

(a) Occlusion distribution map. Brighter region indicates higher occlusion probability

(b) feature X2 and X3 selected by orignial training procedure are replaced by X2' and X3' according to the occlusion probability distribution in each decision node

Figure 5: Proposed method.

head region suffers the least from occlusion. This result conforms with our common sense that the head region is often the most visible part, because most obstacles are located on the ground.

Fig. 5(b) shows how our proposed method impacts the selection of features. Under the original feature selection strategy (Eq. (3)), feature X1, X2 and X3 are selected by the weak classifier. Then we calculate the occlusion distribution map of each splitting node and employ Eq. (4)-(6) to select more robust features. For example, feature X2 is replaced by a more reliable feature X2' which is less likely to be occluded according to the occlusion distribution map. In Fig. 3(c), we see that with the proposed method, the new model is more biased to select the features from the region with low occlusion probability (for example, the head region).

Fig. 4 clearly shows how our proposed method improves the detection of occluded pedestrians. We first introduce occluded pedestrian samples and train the *ACF+occ* model, which shows an improvement of the average miss-rate from 46.53% to 45.64% for the partial occlusion cases (Fig. 4(b)). This demonstrates that the introduction of occluded samples in the training process improves the detection of occluded pedestrians. Unsurprisingly, there is also a reduction of performance in the reasonable case (Fig. 4(a)). However, when we use our method to train the **ACF+occ* model, there is further improvement in both the reasonable and partial occlusion cases. **ACF+occ* successfully eliminates the impact of occlusion samples and achieves a performance comparable to the default *ACF* model for the reasonable case, while in partial occlusion case the average miss rate further reduces to 43.42%.

## 5 OPTIMAL TRAINING AND MORE EXPERIMENTS

Now that we have proposed a new method of utilizing occluded pedestrian samples, in this section we demonstrate its effectiveness with several experiments. The experiments are divided into two parts. In the first part, we exhaustively explore the potential of ACF models and obtain our best detector trained with non-occlusion pedestrian samples. In the second part, we further improve the performance by introducing occluded pedestrians and training them with the proposed method. The evaluation results under different test cases of the Caltech dataset show performances that are better than some state-of-the-art methods.

In both parts of the experiments, we double the default model size to 41×100 pixels, which results in a richer feature of 32×64 pixels per channel. Positive samples in most experiments are obtained by sampling the Caltech video data with a skipping step equal to 10, while a smaller skipping step (more dense sampling) is also used in some cases. We employ some of the modifications proposed in (Ohn-Bar and Trivedi, 2016): a scaling (factor 1.1) is used to augment the number of positive samples by 3 (scaling in horizontal, vertical and both directions), while the randomness handling is also employed to make the

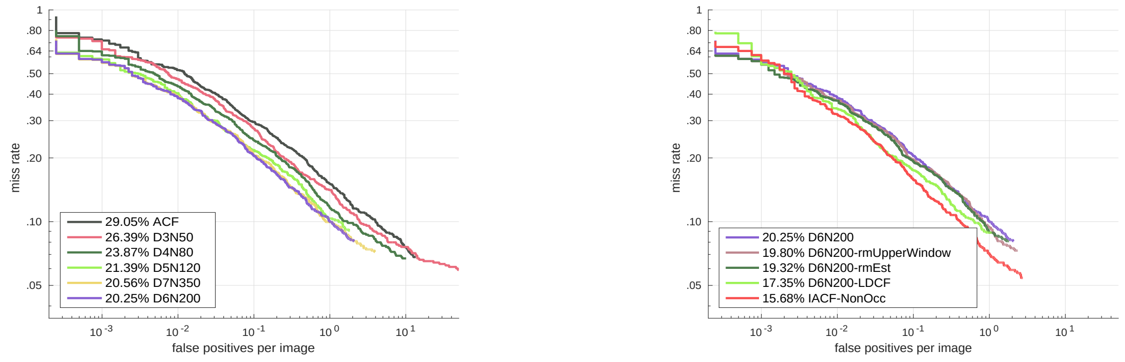

(a) (b)

Figure 6: Performance of models trained with fully visible pedestrian samples.

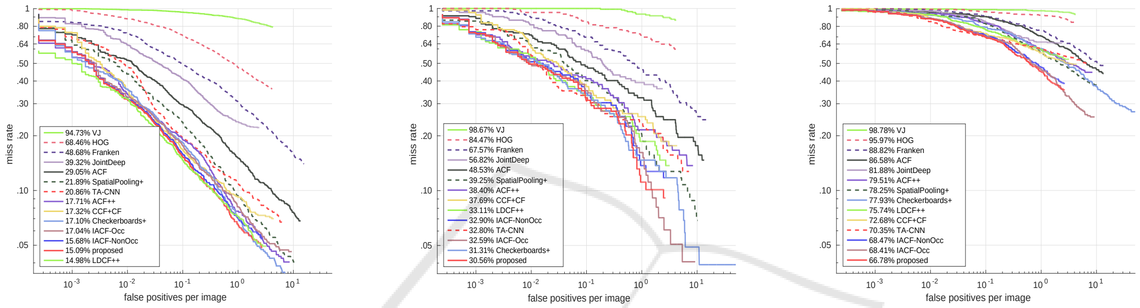

(a) (b) (c)

Figure 7: Comparison with state-of-the-art methods in reasonable, partial occlusion and heavy occlusion cases.

results more reliable.

## 5.1 Training with Non-occlusion Samples

We investigate the optimal training parameters by gradually increasing the maximum depth of the decision trees. For larger model capacity (deeper trees), a bigger collection of training samples is needed to explore the full potential of the model.

We start our experiment with a tree depth equal to 3 and gradually increase the depth to 7 with more training samples (see Fig. 6(a)). At the start, we train a maximum depth 3 model with 50k negative samples, named *D3N50* (D indicates the maximum depth while N indicates negative samples of the model), which already outperforms the ACF detector trained with default settings (maximum depth 5 with 50k negative samples). We conduct multiple experiments to find the optimal data size under a maximum tree depth. When additional data does not lead to an obvious improvement, we consider the model to be saturated. In this way, tree depths from 3 to 7 are evaluated with 50k, 80k, 120k, 200k and 350k negative samples respectively. For deeper trees (depth 6 and 7), more dense sampling with a skipping step of 4 is employed to enlarge the number of positive samples.

In Fig. 6(a) we observe a quick saturation of performance: when the maximum depth reaches 6, additional data seems to help little, even with deeper trees. Thus we fix *D6N200* as our baseline setting and further improve it in Fig. 6(b).

Since the Caltech dataset is captured in the real world, some prior knowledge of the situation can be used. Instead of exhaustively searching the image with sliding windows, we remove those candidates from the upper 1/3 of the image, which obviously reduces the calculation and avoids some false positive detections in the non-pedestrian regions (*D6N200-rmUpperWindow*). Furthermore, we obtain *D6N200-LDCF* and *D6N200-rmEst* by employing feature decorrelation filtering (Nam et al., 2014) and removing feature estimation as suggested in (Ohn-Bar and Trivedi, 2016). With all the above modifications, we obtain our best performance detector trained only with non-occlusion samples named *IACF-NonOcc* (improved ACF detector trained with non-occlusion samples), which is comparable with the state-of-the-art ACF based method LDCF++ (Ohn-Bar and Trivedi, 2016), see Fig. 7(a)).

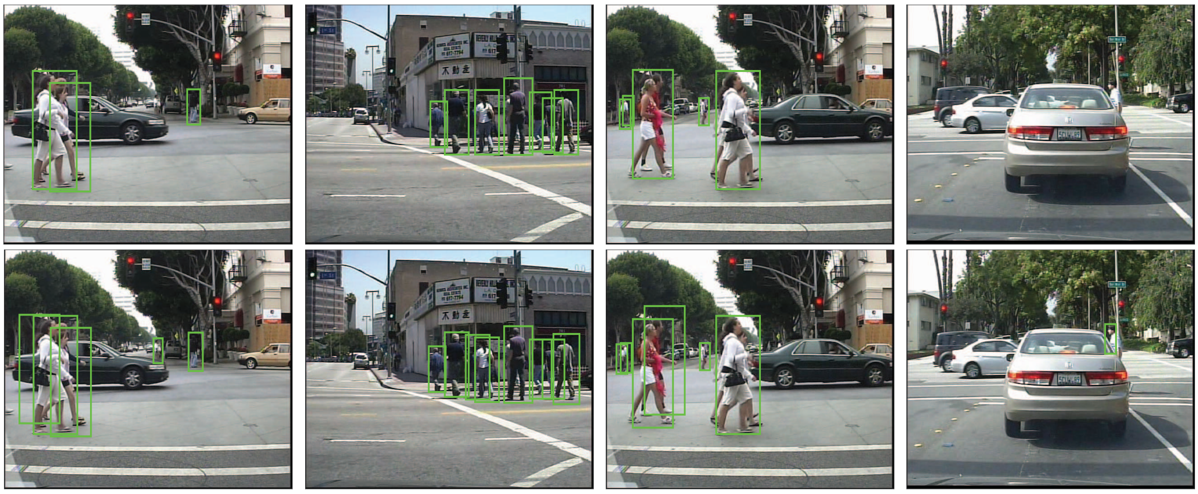

Figure 8: Detection results of *IACF-NonOcc* (first row) and *proposed* (second row) on Caltech Pedestrain dataset. For comparison both the detectors are kept with same number of false positives, while the *proposed* model successfully recognised more occluded pedestrians.

### 5.2 Training with Occluded Samples

In Fig. 7, we evaluate the performance of our models: *IACF-NonOcc*, *IACF-Occ* and *proposed* by comparing with some state-of-the-art methods. The *IACF-NonOcc* is trained only with full-visible pedestrian samples, as explained in Section 5.1. Then we introduce occluded pedestrian samples into the training stage and obtain *IACF-Occ*. In order to show the influence of the occluded samples, all the parameters and modifications of *IACF-NonOcc* are kept unchanged. At last, we achieve the best performance by employing our new training method proposed in Section 4 and get *proposed*.

The methods we use as comparison include *VJ* (Viola and Jones, 2004), *HOG* (Dalal and Triggs, 2005), *Franken* (Mathias et al., 2013), *JointDeep* (Ouyang and Wang, 2013a), *ACF* (Dollár et al., 2014), *SpatialPooling+* (Paisitkriangkrai et al., 2016), *TA-CNN* (Tian et al., 2015), *ACF++* (Ohn-Bar and Trivedi, 2016), *LDCF++* (Ohn-Bar and Trivedi, 2016), *CCF+CF* (Yang et al., 2015) and *Checkerboards+* (Zhang et al., 2015). We obtain the detection results of the above methods from the website of Caltech Pedestrian dataset.

In the commonly used Reasonable case (Fig. 7(a)), unsurprisingly, we observe an obvious performance decline of nearly 2% (15.68% to 17.04%) after we introduce the occluded samples during the training stage (*IACF-Occ*), while the proposed method (*proposed*) successfully eliminates this drop and even slightly outperforms the baseline *IACF-NonOcc* (it reaches 15.09% compared with 15.68%).

The occlusion test cases represent the strong occlusion handling ability of our proposed model. In the partial occlusion case (Fig. 7(b)), the introduction of occluded samples slightly improves the performance from 32.90% to 32.59%, while the proposed model further obtains the best result of 30.56%. More impressive results appear in the heavy occlusion case (Fig. 7(c)), which achieves a significant improvement of nearly 10% (from 75.74% to 66.78%) over the state-of-the-art ACF based model LDCF++, while the efficiency remains the same (only the selected features and thresholds are changed during detection).

Some results of the Caltech Pedestrian dataset are presented in Fig. 8. We observe a more robust detection of occluded pedestrians with our method.

## 6 CONCLUSIONS

This study proposes a novel method to take full advantage of the occluded samples in pedestrian detection. By employing a biased feature selection strategy, the proposed detector shows a significantly enhanced occlusion handling ability.

Since the occlusion distribution map is built on the Caltech Pedestrian dataset, we plan to test its generalization property in other datasets in our future work. But as explained in Section 4.3, this occlusion distribution conforms with the real situation that the lower part of a pedestrian is more likely to be occluded. Therefore, there is reason to believe our method could maintain similar occlusion handling abilities in other datasets of urban situations. What is more, we expect to use our training method in deeper models with a larger size of data to achieve a further improvement.

## REFERENCES

Angelova, A., Krizhevsky, A., Vanhoucke, V., Ogale, A. S., and Ferguson, D. (2015). Real-time pedestrian detection with deep network cascades. In *BMVC*, pages 32–1.

Benenson, R., Mathias, M., Timofte, R., and Van Gool, L. (2012). Pedestrian detection at 100 frames per second. In *Computer Vision and Pattern Recognition (CVPR), 2012 IEEE Conference on*, pages 2903–2910. IEEE.

Benenson, R., Mathias, M., Tuytelaars, T., and Van Gool, L. (2013). Seeking the strongest rigid detector. In *Proceedings of the IEEE Conference on Computer Vision and Pattern Recognition*, pages 3666–3673.

Dalal, N. and Triggs, B. (2005). Histograms of oriented gradients for human detection. In *Computer Vision and Pattern Recognition, 2005. CVPR 2005. IEEE Computer Society Conference on*, volume 1, pages 886–893. IEEE.

Dollár, P., Appel, R., Belongie, S., and Perona, P. (2014). Fast feature pyramids for object detection. *IEEE Transactions on Pattern Analysis and Machine Intelligence*, 36(8):1532–1545.

Dollár, P., Belongie, S. J., and Perona, P. (2010). The fastest pedestrian detector in the west. In *BMVC*, volume 2, page 7.

Dollár, P., Tu, Z., Perona, P., and Belongie, S. (2009). Integral channel features.

Dollar, P., Wojek, C., Schiele, B., and Perona, P. (2012). Pedestrian detection: An evaluation of the state of the art. *IEEE transactions on pattern analysis and machine intelligence*, 34(4):743–761.

Enzweiler, M., Eigenstetter, A., Schiele, B., and Gavrila, D. M. (2010). Multi-cue pedestrian classification with partial occlusion handling. In *Computer vision and pattern recognition (CVPR), 2010 IEEE Conference on*, pages 990–997. IEEE.

Felzenszwalb, P. F., Girshick, R. B., McAllester, D., and Ramanan, D. (2010). Object detection with discriminatively trained part-based models. *IEEE transactions on pattern analysis and machine intelligence*, 32(9):1627–1645.

Friedman, J., Hastie, T., Tibshirani, R., et al. (2000). Additive logistic regression: a statistical view of boosting (with discussion and a rejoinder by the authors). *The annals of statistics*, 28(2):337–407.

Mathias, M., Benenson, R., Timofte, R., and Van Gool, L. (2013). Handling occlusions with franken-classifiers. In *Proceedings of the IEEE International Conference on Computer Vision*, pages 1505–1512.

Nam, W., Dollár, P., and Han, J. H. (2014). Local decorrelation for improved detection. *Eprint Arxiv*.

Ohn-Bar, E. and Trivedi, M. M. (2016). To boost or not to boost? on the limits of boosted trees for object detection. In *Pattern Recognition (ICPR), 2016 23rd International Conference on*, pages 3350–3355. IEEE.

Ouyang, W. and Wang, X. (2013a). Joint deep learning for pedestrian detection. In *Proceedings of the IEEE International Conference on Computer Vision*, pages 2056–2063.

Ouyang, W. and Wang, X. (2013b). Single-pedestrian detection aided by multi-pedestrian detection. In *Proceedings of the IEEE Conference on Computer Vision and Pattern Recognition*, pages 3198–3205.

Ouyang, W., Zeng, X., and Wang, X. (2016). Partial occlusion handling in pedestrian detection with a deep model. *IEEE Transactions on Circuits and Systems for Video Technology*, 26(11):2123–2137.

Paisitkriangkrai, S., Shen, C., and van den Hengel, A. (2016). Pedestrian detection with spatially pooled features and structured ensemble learning. *IEEE transactions on pattern analysis and machine intelligence*, 38(6):1243–1257.

Tang, S., Andriluka, M., and Schiele, B. (2014). Detection and tracking of occluded people. *International Journal of Computer Vision*, 110(1):58–69.

Tian, Y., Luo, P., Wang, X., and Tang, X. (2015). Pedestrian detection aided by deep learning semantic tasks. In *Proceedings of the IEEE Conference on Computer Vision and Pattern Recognition*, pages 5079–5087.

Viola, P. and Jones, M. J. (2004). Robust real-time face detection. *International journal of computer vision*, 57(2):137–154.

Walk, S., Majer, N., Schindler, K., and Schiele, B. (2010). New features and insights for pedestrian detection. In *Computer vision and pattern recognition (CVPR), 2010 IEEE conference on*, pages 1030–1037. IEEE.

Wang, X., Han, T. X., and Yan, S. (2009). An hog-lbp human detector with partial occlusion handling. In *Computer Vision, 2009 IEEE 12th International Conference on*, pages 32–39. IEEE.

Wojek, C., Walk, S., Roth, S., and Schiele, B. (2011). Monocular 3d scene understanding with explicit occlusion reasoning. In *Computer Vision and Pattern Recognition (CVPR), 2011 IEEE Conference on*, pages 1993–2000. IEEE.

Yang, B., Yan, J., Lei, Z., and Li, S. Z. (2015). Convolutional channel features. In *Proceedings of the IEEE international conference on computer vision*, pages 82–90.

Zhang, S., Benenson, R., and Schiele, B. (2015). Filtered channel features for pedestrian detection. In *Computer Vision and Pattern Recognition (CVPR), 2015 IEEE Conference on*, pages 1751–1760. IEEE.